An Automatic Pin Identification Method for a Three-Phase DC Brushless Motor

Shyh-Jier Wang[2], Chi-Chang Cheng[1], Shir-Kuan Lin[1], Jau-Jiu Ju[2], and Der-Ray Huang[2]

[1]Department of Electrical and Control Engineering, National Chiao Tung University, Hsinchu 300, Taiwan
[2]Magnetics Department, Opto-Electronics and Systems Laboratories, Industrial Technology Research Institute, Hsinchu 310, Taiwan

The pin identification is to find the definition of each connecting pin of a three-phase brushless motor. The 11 pins of the motor can be distinguished into three groups by a simple resistance measurement method. An automatic method has two steps. In the first step, the motor is in an open-circuited mode; and the individual pins of the windings are identified by comparing back electromotive forces. A special integral is defined and used to match Hall signal pins with the Hall sensors. The polarity of each pair of the Hall signal pins is determined by the second step of a standstill method. The proposed method is illustrated and verified by an experiment.

***Index Terms*—Identification, Lyapunov stability, motor characteristics, three-phase dc brushless motor.**

I. Introduction

THREE-PHASE dc brushless motors (DCBM) have been used broadly in electronic apparatuses. The technicians often want to test the performance or measure the parameters of a motor [1]–[3]. Instead of the inconvenient way to search the data sheets of motors or to ask the motor manufacturers, most technicians would rather use an inefficient trial-and-error method to determine the pin assignment themselves. Little literature investigated such a practical problem. This paper tries to provide an automatic identification to determine the correct pin assignment of a DCBM motor, which is desired in industry. The salient features are the definition of a special integral and the steady-state determination of a dc current excitation. The special integral provides a useful electrical property that only three cases of signal combinations are not divergent, which is used to determine the relationship between the pins of Hall sensors and those of current windings.

II. Three Groups

There are 11 pins in a DCBM, which can be categorized into three groups: A) three terminal pins of armature windings; B) two power pins of three Hall sensors; C) six signal pins of three Hall sensors. The three pins in group A are denoted by pins of v_a, v_b, and v_c, since they are also used to measure the voltages (v_a, v_b, and v_c) of winding terminals of phases a, b, and c with respect to the ground. The power pins H^+ and H^- in group B are, respectively, connected to the positive and negative terminals of a dc supply. There are three pairs in group C, each has two signal pins of a Hall sensor, e.g., pins of h_a^+ and h_a^- are two signal terminals of Hall sensor H_a. The polarity of the power pins H^+ and H^- is not critical. The reverse assignment makes the polarity of each pair of Hall signal pins reverse only.

Any pin in group A is not connected with pins of groups B and C, and can be easily picked out by measuring the resistance between any two pins. It is assumed that three Hall sensors have the same properties, so that the resistance between two signal pins of every Hall sensor is almost the same. On the other hand, the resistance between one signal pin of a Hall sensor and any one pin of another Hall sensor is little different for different Hall sensors. This observation allows us to distinguish group B from group C. Table I shows the resistance between every two pins of a typical DCBM motor. It is apparent that pins 9–11 belong to group A, while the others are either in group B or in group C. The resistances of pin 1 with pins 2–8 indicate that pins 1 and 8 are the power pins H^+ and H^- in group B, since the other six resistances are almost the same. The resistance of pins 2 and 3 is different from those of pin 2 with pins 4–7, it can be concluded that pins 2 and 3 are a pair of signal pins of a Hall sensor, and so are pins 4 and 5 and pins 6 and 7.

TABLE I
Resistances Between any Two Pins (in Ω)

Pin	1	2	3	4	5	6	7	8	9	10	11
1	—	243	240	236	240	230	228	109	∞	∞	∞
2	243	—	332	423	426	416	414	241	∞	∞	∞
3	240	332	—	420	423	413	411	238	∞	∞	∞
4	236	423	420	—	328	409	407	235	∞	∞	∞
5	240	426	423	328	—	420	415	241	∞	∞	∞
6	230	416	413	409	420	—	318	232	∞	∞	∞
7	228	414	411	407	415	318	—	230	∞	∞	∞
8	109	241	238	235	241	232	230	—	∞	∞	∞
9	∞	∞	∞	∞	∞	∞	∞	∞	—	3.9	3.9
10	∞	∞	∞	∞	∞	∞	∞	∞	3.9	—	3.9
11	∞	∞	∞	∞	∞	∞	∞	∞	3.9	3.9	—

After 11 pins are distinguished into three groups and the polarity of the power pins in group B is assigned, the pin identification turns out to be the determination of individual pins of v_a, v_b, and v_c, the matching of pairs of pins in group C with the Hall sensors $\mathrm{H}_a, \mathrm{H}_b$, and H_c, and the polarity determination of each pair in group C. This paper proposes three ways to solve these three problems, respectively.

III. Theory

Consider a DCBM with three-phase and Y-connected windings, whose model can be described as [4]

$$\begin{bmatrix} v_{as} \\ v_{bs} \\ v_{cs} \end{bmatrix} = r_s \begin{bmatrix} i_a \\ i_b \\ i_c \end{bmatrix} + \begin{bmatrix} L_s & -M & -M \\ -M & L_s & -M \\ -M & -M & L_s \end{bmatrix} \begin{bmatrix} \dot{i}_a \\ \dot{i}_b \\ \dot{i}_c \end{bmatrix} + \frac{\mathrm{d}\theta_r}{\mathrm{d}t} \lambda_r \begin{bmatrix} \cos\theta_r \\ \cos\left(\theta_r - \frac{2\pi}{3}\right) \\ \cos\left(\theta_r + \frac{2\pi}{3}\right) \end{bmatrix} \quad (1)$$

Digital Object Identifier 10.1109/TMAG.2005.854970

where v_{as}, v_{bs}, and v_{cs}, are the terminal voltages with respect to the neutral point s, i_a, i_b, and i_c are the currents of phases a, b, c, respectively, r_s is the winding resistance per phase, L_s is the self inductance per phase, M is the mutual inductance per phase, λ_r is the maximum flux induced by the rotor magnet, and θ_r is the rotational electrical angle of the rotor. Note that $\theta_r = 0$ is the position where the intersection line of the N-S and the S-N magnet is in alignment with the center line of a tooth of phase a [5]. Furthermore, the output torque T_e of the motor can be obtained as [4]

$$T_e = \frac{P}{2}\lambda_r \left[\left(i_a - \frac{i_b}{2} - \frac{i_c}{2} \right) \cos\theta_r + \frac{\sqrt{3}}{2}(i_b - i_c)\sin\theta_r \right] \tag{2}$$

where P is the number of poles of the magnet. On the other hand, the dynamics of the DCBM can be described as

$$\frac{2J}{P}\frac{d^2\theta_r}{dt^2} + \frac{2B_m}{P}\frac{d\theta_r}{dt} = T_e - T_L \tag{3}$$

where J is the inertia, B_m is the damping ratio, and T_L is the loading torque. For simplicity, it is assumed that $T_L = 0$ in the following.

A. Winding Determination by Back Electromotive Forces (EMFs)

When the motor is in an open-circuited mode, i.e., $i_a = i_b = i_c = 0$, the voltage between a winding terminal and the neutral point is the back EMFs of a phase. It can be obtained from (1) by letting $i_a(t) = i_b(t) = i_c(t) = 0$ that the back EMFs of phases a, b, and c are, respectively

$$e_a \equiv v_{as} = \lambda_r \frac{d\theta_r}{dt}\cos\theta_r \tag{4}$$

$$e_b \equiv v_{bs} = \lambda_r \frac{d\theta_r}{dt}\cos\left(\theta_r - \frac{2\pi}{3}\right) \tag{5}$$

$$e_c \equiv v_{cs} = \lambda_r \frac{d\theta_r}{dt}\cos\left(\theta_r + \frac{2\pi}{3}\right). \tag{6}$$

It follows from (4)–(6) that $v_{as} + v_{bs} + v_{cs} = 0$ in the open-circuited mode. It is known that $v_{as} + v_{bs} + v_{cs} = v_a + v_b + v_c - 3v_s$, where v_a, v_b, and v_c are the terminal voltages with respect to a common reference (e.g., ground). Thus, $v_{as} = v_a - (v_a + v_b + v_c)/3$, etc. The back EMFs e_a, e_b, and e_c can then be calculated out using the measured values of v_a, v_b, and v_c.

It is evident from (4)–(6) that $e_a = 0, e_b < 0$, and $e_c > 0$ when $d\theta_r/dt > 0$ and $\theta_r = 3\pi/2 + 2n\pi$ for any integer n. This provides a rule to determine the phase of each winding terminal.

B. Hall Sensors

The three Hall sensors are installed to measure the rotor flux linkage, and the Hall sensor H_a is so arranged [5] that its output h_a (the voltage difference of the positive (h_a^+) and negative (h_a^-) terminals of the sensor: $h_a = h_a^+ - h_a^-$) is proportional to $\sin(\theta_r + 2\pi/3) = -\cos(\theta_r + \pi/6)$. As a result

$$\begin{aligned} h_a \equiv h_a^+ - h_a^- &= -v_o \cos\left(\theta_r + \frac{\pi}{6}\right) \\ &= v_o \cos\left(\theta_r - \frac{5\pi}{6}\right) \end{aligned} \tag{7}$$

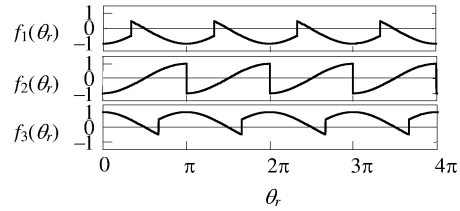

Fig. 1. Functions of $f_1(\theta_r) \equiv \cos\theta_r \mathrm{sign}[\cos(\theta_r - 5\pi/6)], f_2(\theta_r) \equiv \cos\theta_r \mathrm{sign}[\cos(\theta_r + \pi/2)], f_3(\theta_r) \equiv \cos\theta_r \mathrm{sign}[\cos(\theta_r - \pi/6)]$.

$$\begin{aligned} h_b \equiv h_b^+ - h_b^- &= -v_o \cos\left(\theta_r - \frac{2\pi}{3} + \frac{\pi}{6}\right) \\ &= v_o \cos\left(\theta_r + \frac{\pi}{2}\right) \end{aligned} \tag{8}$$

$$\begin{aligned} h_c \equiv h_c^+ - h_c^- &= -v_o \cos\left(\theta_r + \frac{2\pi}{3} + \frac{\pi}{6}\right) \\ &= v_o \cos\left(\theta_r - \frac{\pi}{6}\right) \end{aligned} \tag{9}$$

where $v_o > 0$ is the amplitude.

Comparing (4) with (7)–(9) reveals that e_a leads h_a and h_c by $5\pi/6$ and $\pi/6$, respectively, whereas e_a lags h_b by $\pi/2$. This motivates us to define an integral $\Psi_{\mathrm{ij}} \equiv \int_0^t e_i(\tau)\mathrm{sign}[h_j(\tau)]d\tau$, where subscripts i and j are a, b, or c. It can be shown [6] that

$$\begin{aligned} \Psi_{aa} &= \lambda_r \int_{\theta_r(0)}^{\theta_r(t)} \cos\theta_r \mathrm{sign}\left[\cos\left(\theta_r - \frac{5\pi}{6}\right)\right] d\theta_r \\ &\to -\infty \quad \text{as} \quad t \to \infty \end{aligned} \tag{10}$$

$$\Psi_{ab} = \lambda_r \int_{\theta_r(0)}^{\theta_r(t)} \cos\theta_r \mathrm{sign}\left[\cos\left(\theta_r + \frac{\pi}{2}\right)\right] d\theta_r \tag{11}$$

$$\begin{aligned} \Psi_{ac} &= \lambda_r \int_{\theta_r(0)}^{\theta_r(t)} \cos\theta_r \mathrm{sign}\left[\cos\left(\theta_r - \frac{\pi}{6}\right)\right] d\theta_r \\ &\to -\infty \quad \text{as} \quad t \to \infty. \end{aligned} \tag{12}$$

It should be remarked that the integrands in (10)–(12) are all periodic functions of θ_r, as shown in Fig. 1. Ψ_{ab} is bounded and close to zero since it is zero for $\theta_r\ (t) = \theta_r(0) + n\pi$. On the contrary, Ψ_{aa} and Ψ_{ac} have, respectively, negative and positive values for the integration over any period, i.e., $\theta_r(t) = \theta_r(0) + \pi$, so that both are either an increasing or a decreasing function. Similar results can be obtained for the other Ψ_{ij}. Consequently, only Ψ_{ab}, Ψ_{bc} and Ψ_{ca} are bounded, the others increase or decrease with time. These integral phenomena allow us to match each individual Hall sensor with its corresponding winding without knowing the polarities of the Hall sensors *a priori*. For instance, Hall sensor H_b can be determined by recognizing Ψ_{ab}.

C. Polarity of a Hall Sensor

Examine (7)–(9) again, we find that the output values of three Hall sensors are fixed for a fixed θ_r. If the motor is held stationary at $\theta_r = 5\pi/6 + 2n\pi$, then h_a must be greater than zero, while both h_b and h_c must be less than zero, i.e., $h_a > 0, h_b < 0$, and $h_c < 0$. Whenever the measured output of a Hall sensor is not consistent with this condition, the polarity of the signals of the Hall sensor should be reversely assigned.

If the windings of phases a and b are connected with a dc source and the other winding is grounded, then $i_a = i_b = i/2$

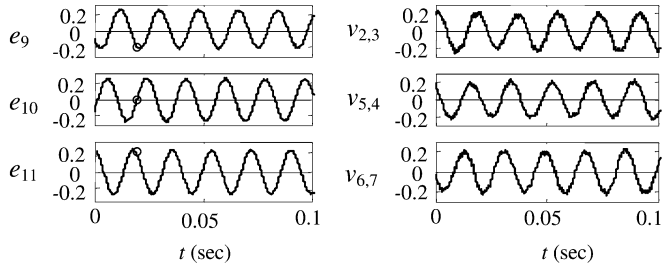

Fig. 2. Voltage histories (in V) of $e_9, e_{10}, e_{11}, v_{2,3} = v_2 - v_3, v_{5,4} = v_5 - v_4$, and $v_{6,7} = v_6 - v_7$.

and $i_c = -i$, where $i > 0$. Substituting these currents into (2) yields

$$T_e = \frac{3P}{4}\lambda_r i \sin\left(\theta_r + \frac{\pi}{6}\right). \tag{13}$$

Combining (3) and (14) leads to the state equation of

$$\dot{\mathbf{x}} = \mathbf{f}(\mathbf{x}, i) = \begin{bmatrix} x_2 \\ -\frac{B_m}{J}x_2 + \frac{3P^2}{8J}\lambda_r i \sin(x_1 + \pi/6) \end{bmatrix} \tag{14}$$

where $\mathbf{x} = [x_1, x_2]^t$ is the vector of the state variables $x_1 = \theta_r$ and $x_2 = dx_1/dt = d\theta_r/dt$. There are two equilibrium points $\mathbf{x}_{e1} = [5\pi/6, 0]^t$ and $\mathbf{x}_{e2} = [-\pi/6, 0]^t$ since $\mathbf{f}(\mathbf{x}_{e1}, i) = \mathbf{f}(\mathbf{x}_{e2}, i) = \mathbf{0}$. It can be shown by the Lyapunov stability theory [7] that the equilibrium $\mathbf{x}_{e1} = [5\pi/6, 0]^t$ is uniformly asymptotically stable for $i > 0$ (a similar proof can be found in [5]). $\theta_r = 5\pi/6 + 2n\pi$ is then the steady-state for $i_a = i_b = i/2$ and $i_c = -i < 0$, at which $h_a > 0, h_b < 0$, and $h_c < 0$.

IV. Experimental Verification

A DCBM used as a spindle motor of a $50\times$ CD-ROM is taken as an experimental target. Table I already shows the resistances between any two pins of the motor. Pins 1 and 8 are assigned as the power pins H^+ and H^-, respectively, and are connected to a dc power supply (5 V). It is known that pins 9–11 are pins in group A, while pins 2 and 3, pins 4 and 5, and pins 6 and 7 are three pairs in group C.

A. Step 1

The motor is pushed to rotate by hand and the voltage histories of pins 2–7 and 9–11 are recorded and shown in Fig. 2, where v_i is the voltage of pin $i, v_{i,j} = v_i - v_j$, and $e_k = v_k - (v_9 + v_{10} + v_{11})/3$ for $k = 9, 10$, and 11. Define $\Psi_{k(i,j)} \equiv \int_0^t e_k(\tau)\mathrm{sign}[v_{i,j}(\tau)]\,d\tau$. The histories of $\Psi_{9(i,j)}$ and $\Psi_{10(i,j)}$ are plotted in Fig. 3.

- Assign pin 10 as the pin of v_a. It can be seen in Fig. 2 that $e_9 < 0$ and $e_{11} > 0$ when e_{10} crosses 0 from 0^- to 0^+ (i.e., $\theta_r = 3\pi/2 + 2n\pi$). This implies that pins 9 and 11 are the pins of v_b and v_c, respectively.
- Since $\Psi_{9(2,3)} = \Psi_{b(2,3)}$ and $\Psi_{10(6,7)} = \Psi_{a(6,7)}$ are close to zero (they also go slightly away from 0 due to numerical errors), the pair of pins 6 and 7 is that of the Hall sensor H_b, while the pair of pins 2 and 3 is that of the Hall sensor H_c. Consequently, the pair of the Hall sensor H_a consists of pins 4 and 5.

B. Step 2

Supply the winding currents as $i_a = i_b = i/2$ and $i_c = -i$, where $i = 0.5$ A. The voltage histories of v_{23}, v_{54}, and v_{67} are recorded and shown in Fig. 4.

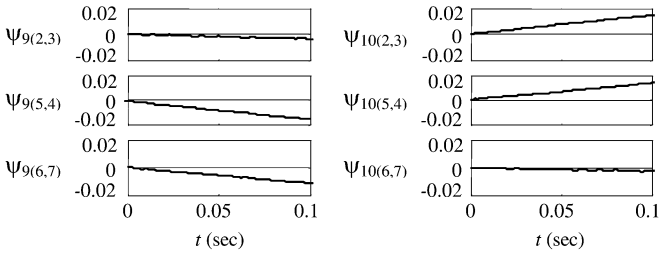

Fig. 3. Integral histories (in $\mathrm{V}\cdot\mathrm{s}$) of $\Psi_{9(2,3)}, \Psi_{9(5,4)}, \Psi_{9(6,7)}, \Psi_{10(2,3)}, \Psi_{10(5,4)}$, and $\Psi_{10(6,7)}$.

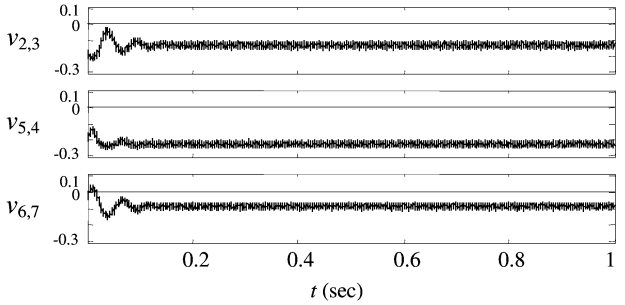

Fig. 4. The Hall sensor outputs (in V) in the standstill mode: $i_a = i_b = i/2$ and $i_c = -i$ with $i = 0.5$ A.

- $h_a = -v_{5,4}, h_b = v_{6,7}$, and $h_c = v_{2,3}$, since $v_{2,3} < 0, v_{5,4} < 0$, and $v_{6,7} < 0$, but we know that $h_a > 0, h_b < 0$, and $h_c < 0$ at the steady-state. Therefore, pins 2–7 are pins of $h_c^+, h_c^-, h_a^+, h_a^-, h_b^+, h_b^-$, respectively.

V. Conclusion

The proposed automatic method to identify the pin assignment has been experimentally illustrated in Section IV. To verify the result, we also connected the motor to a CD-ROM driver chip BA6849 in accordance with the identified pin assignment, and found that the motor rotated normally.

Acknowledgment

This work was supported in part by the National Science Council, Taiwan, under Grant NSC 93-2218-E-009-034.

References

[1] C. Delecluse and D. Grenier, "A measurement method of the exact variations of the self and mutual inductances of a buried permanent magnet synchronous motor and its application to the reduction of torque ripples," in *Proc. 5th Int. Workshop Advanced Motion Control*, 1998, pp. 191–197.

[2] T. Takaharu and M. Nobuyuki, "Sensorless brushless dc motor drive with EMF constant identifier," *Proc. IECON*, vol. 1, pp. 14–19, 1994.

[3] T. Hisashi, K. Takashi, and T. Hirokazu, "Real-time estimation method of brushless dc servomotor parameters," in *Proc. Power Conversion Conf.*, vol. 2, 1997, pp. 673–678.

[4] D. W. Novotny and T. A. Lipo, *Vector Control and Dynamics of AC Drivers*. New York, : Oxford, 1996.

[5] S. J. Wang and S. K. Lin, "Inductances and resistance measurement of a permanent magnet synchronous motor," in *Proc. World Congr. Intell. Control Autom.*, Hangzhou, Zhejiang, China, 2004, pp. 4391–4395.

[6] G. B. Folland, *Advanced Calculus*. Englewood Cliffs, NJ: Prentice-Hall, 2002.

[7] M. Vidyasagar, *Nonlinear Systems Analysis*, 2nd ed. Englewood Cliffs, NJ: Prentice-Hall, 1993.

Manuscript received February 7, 2005.